ISSN 0208-7774 TRIBOLOGIA 5/2020 p. 39–50
DOI: 10.5604/01.3001.0014.6957

Wojciech RYNIEWICZ*, **Anna M. RYNIEWICZ****, **Łukasz BOJKO*****, **Konrad MAZUR******

THE SIMULATION ASSESSMENT OF THE VENEERING LAYERS OF PROSTHETIC CROWNS IN CONCENTRATED CONTACT

SYMULACYJNA OCENA WARSTW LICUJĄCYCH KORONY PROTETYCZNE W STYKU SKONCENTROWANYM

Key words: prosthetic restorations, layered materials, FEM simulation.

Abstract: The aim of the study is to simulate and analyse the distributions of stresses and resultant displacements during concentrated loading of the layered material compositions used in prosthetic crowns in order to assess their resistance and demonstrate the impact of strength parameters of the veneer and framework on the transfer of external loads. The research materials are samples replicating the layered structure of prosthetic crowns. The load-bearing layers were made using CAD/CAM technology, and the dedicated veneering layers were fired or polymerized on the frameworks and constituted the top structure for cooperation during occlusion. If the material of the veneering layer differs from the material building the framework, for example, in the ceramic-metal type, spreading of the resultant displacements to the framework and high values of shear stress at the border of the veneering layer and the framework may be unfavourable and cause the veneer layer to chip off. This distribution of stresses and displacements may have a much smaller impact on the ceramic veneering of a ceramic or glass-ceramic framework, as both layers are much more homogeneous in terms of material.

Słowa kluczowe: konstrukcje protetyczne, materiały warstwowe, symulacja MES.

Streszczenie: Celem pracy jest symulacja i analiza procesu rozchodzenia się naprężeń i przemieszczeń w trakcie skoncentrowanego obciążenia warstwowych kompozycji materiałowych stosowanych w koronach protetycznych, która pozwala na ocenę ich odporności oraz wykazanie wpływu parametrów wytrzymałościowych licowania i podbudowy na przenoszenie obciążeń zewnętrznych. Materiałem badań są próbki replikujące warstwową budowę koron protetycznych. Warstwy nośne zostały wytworzone w technologii CAD/CAM, a dedykowane warstwy licujące były napalane lub polimeryzowane na podbudowach i stanowiły wierzchnią strukturę do współpracy w warunkach okluzji. W przypadku zróżnicowania materiałowego warstwy licowania od podbudowy, typu ceramika – metal, zjawiska rozprzestrzeniania się przemieszczeń wypadkowych do podbudowy oraz duże wartości naprężeń stycznych na granicy warstwy licującej i podbudowy mogą być niekorzystne i powodować odpryskiwanie warstwy licującej. Taki rozkład naprężeń i przemieszczeń może w znacznie mniejszym stopniu oddziaływać na licowanie ceramiką podbudowy ceramicznej lub szklanoceramicznej, ponieważ obie warstwy są znacznie bardziej jednorodne materiałowo.

INTRODUCTION

Prosthetic crowns are used to rebuild the crowns of natural teeth that were significantly damaged. They can be a solution for a single tooth or the attachment of more extensive fixed restorations – prosthetic bridges. In addition to prosthetic crowns serving as fastening elements, the bridge consists of a span that replaces lost teeth. Crowns and bridges are made in accordance with the rules of clinical procedures and while taking into

* ORCID: 0000-0002-9140-198X. Jagiellonian University Medical College, Faculty of Medicine, Dental Institute, Department of Dental Prosthodontics, Montelupich 4 Street, 31-155 Cracow, Poland.
** ORCID: 0000-0003-2469-6527. Jagiellonian University Medical College, Faculty of Medicine, Dental Institute, Department of Dental Prosthodontics, Montelupich 4 Street, 31-155 Cracow, Poland.
*** ORCID: 0000-0002-6024-458X. AGH University of Science and Technology, Faculty of Mechanical Engineering and Robotics, Mickiewicza 30 Ave., 30-059 Cracow, Poland.
**** AGH University of Science and Technology, Faculty of Mechanical Engineering and Robotics, Mickiewicza 30 Ave., 30-059 Cracow, Poland.

account the principles of strength, biocompatibility, and aesthetics **[L. 1–5]**. The restoration should ensure, similar to physiological, the transfer of occlusive loads and resistance to loads in the contact between the structures of the masticatory organ. The load-bearing framework of the crown or bridge is veneered, depending on the biomaterial and the production technology. Ceramic veneering layers of the framework for fixed prosthetic restorations are responsible for the direct functional and tribological cooperation with the opposing teeth and for the transfer of contact loads.

This topic is important due to the introduction of new biomaterials in modern prosthetics as well as the application of the CAD/CAM system for the design and production of load-bearing structures. This involves the need to use new procedures, targeted veneering, and the assessment of the impact of strength parameters of the layered materials on the interaction between the elements **[L. 3, 6–13]**.

The aim of the study is to simulate and analyse the distributions of stresses and resultant displacements during concentrated loading of the layered material compositions used in prosthetic crowns, produced on metal, glass-ceramic, ceramic, and polymer frameworks, in order to assess their resistance and demonstrate the impact of strength parameters of the veneer and framework on the transfer of external loads.

RESEARCH MATERIAL

The research material included dedicated ceramic adhesive systems with veneer frameworks: metal made of CoCrMo, TiCP, Ti6Al4V; glass-ceramic made of $LiSi_2$; and, a ceramic made of ZrO_2 and composite veneering polymer framework made of polyether ether ketone (PEEK). A natural enamel-dentin junction was used as the layered control structure. The samples of materials for load-bearing frameworks, in the form of 6.35 mm discs with a thickness of 2 mm, 9 pieces each, were made of factory matrices using the milling technology in a CAD/CAM system. The veneering layer on the discs was 1 mm thick. The procedure for making a layered structure for fixed dentures depends on the type of material of the framework, the technology of the preparation, and the subsequent stages of applying and firing the opaque, dentin, and enamel layers. In the case of PEEK framework, the veneering layer made of the composite material is hardened by LED light. The material combination of composite – PEEK was used in simulation studies due to the possibility of analysing the framework with a low elasticity modulus. **Table 1** shows layered structures chosen for the research, which were made in the form of discs and dedicated for the FEM simulation experiment. The strength parameters of the veneering layer and the framework as well as the friction coefficients between the indenter and the veneer layer have been determined **[L. 14]**.

Table 1. Layered material compositions of the veneering layer–framework type used in the production of fixed restorations [L. 14–18]

Tabela 1. Warstwowe kompozycje materiałowe typu warstwa licująca–podbudowa stosowane w konstrukcjach protez stałych **[L. 14–18]**

Number	Layered material composition		Young's modulus E, GPa	Poisson's ratio, ν	Coefficient of friction
1	Veneering layer	Duceram Kiss	65	0.28	–
	Framework	CoCrMo	203.8	0.29	0.68
2	Veneering layer	Vita Titankeramik	91	0.28	–
	Framework	TiCP	108	0.35	0.60
3	Veneering layer	Vita Titankeramik	91	0.28	–
	Framework	Ti6Al4V	115.2	0.34	0.65
4	Veneering layer	IPS e.max Ceram	95	0.24	–
	Framework	$LiSi_2$	95	0.20	0.58
5	Veneering layer	Elephant Sakura	60	0.265	–
	Framework	ZrO_2	210	0.30	0.72
6	Veneering layer	Composite	15	0.30	–
	Framework	PEEK	3.5	0.36	0.20
7	Enamel		84.1	0.33	–
	Dentine		18.6	0.32	0.50

RESEARCH METHOD

The research method was based on modelling the process of indentation with the use of a diamond indenter in the shape of a regular tetrahedron with an opening angle of 136°, which was virtually pressed into the layered materials (**Fig. 1**).

The research node model and numerical analysis were performed using the Ansys Workbench software. Constant contact was adopted between the veneering layer and the framework. The free surface of the framework was fixed, and the indenter, which was placed centrally in relation to the disc, in subsequent tests was axially loaded as follows: in the first series 5 N and in the second series 20 N. The strength parameters of the biomaterials and tissues were adopted as isotropic. Assuming elastic deformations, the simulations were performed with the use of Young's modulus and Poisson's ratio for two-layer discs. The friction coefficients between the indenter and the veneering layer were also adopted. Discretization included the areas where the stress concentration was expected. The mesh was compacted in the area of contact between the indenter and the veneering layer. Tetrahedral elements were used to discretize the system.

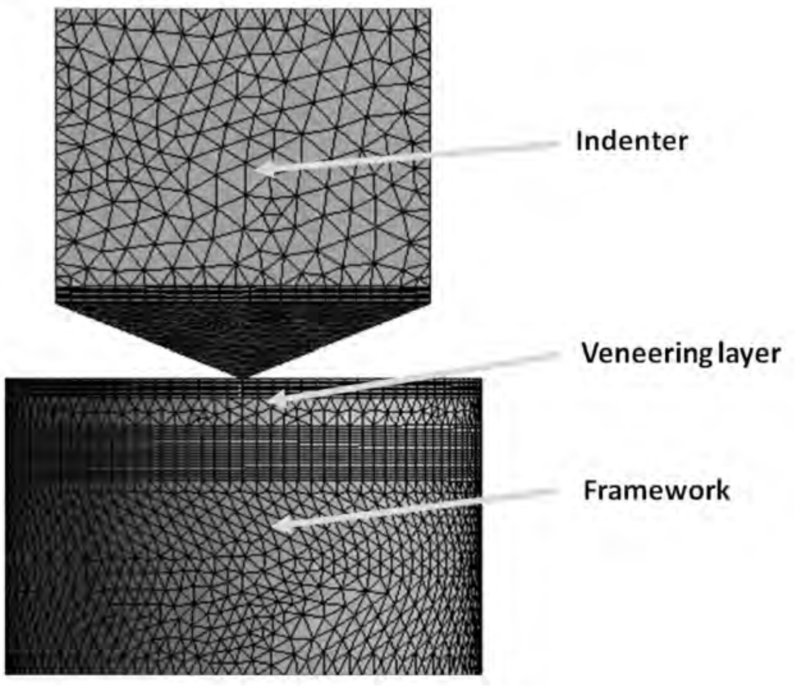

Fig. 1. Model for simulation examinations of the layered biomaterials
Rys. 1. Model do badań symulacyjnych biomateriałów warstwowych

SIMULATION RESULTS AND DISCUSSION

The results of the calculations are presented in the form of maps of the distribution of reduced stresses in the tested models according to the Huber-Mises-Hencky (HMH) hypothesis, shear stresses determined at the border of the veneering layer and the framework, as well as resultant displacements in layered material compositions. Distribution maps for a load of 5 N are shown in **Figures 2, 4, 6, 8, 10, 12,** and **14**, and for a load of 20N in **Figures 3, 5, 7, 9, 11, 13,** and **15**. Due to the different values of stresses and displacements, automatically generated scales were used on the maps of distribution.

In the model with veneering the CoCrMo framework with Duceram Kiss ceramics and an indenter load of 5 N, the reduced stresses are located in the veneering layer and framework, with a characteristic expansion after transition to the framework. In the veneering layer, the values range from 88.58 MPa – the maximum value, to 2 MPa (**Fig. 2a**). At the boundary of the layer connection, the stresses have the values of 2–8 MPa. After transition to the CoCrMo framework, the values reach the minimum of 0.0009 MPa. The shear stresses in the connection zone of the veneering layer and the framework range from -0.26 MPa to 0.29 MPa (**Fig. 2b**). The resultant displacements with a maximum value of 0.41 μm are located only in the veneering layer (**Fig. 2c**). With such a configuration of the strength parameters for the veneering layer and framework, a limited spread of displacements was found in the veneering layer. Perhaps this is a favourable phenomenon ensuring good adhesion of the veneering ceramics to the framework.

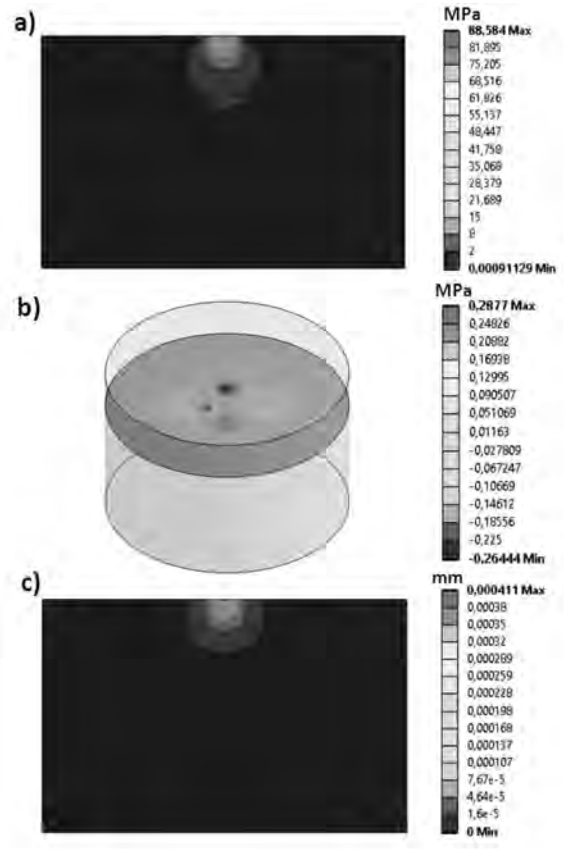

Fig. 2. Duceram Kiss-CoCrMo connection loaded with a force of 5 N: a) reduced stresses, b) shear stresses at the border of connection, c) resultant displacements

Rys. 2. Połączenie Duceram Kiss-CoCrMo obciążone siłą 5 N: a) naprężenia zredukowane, b) naprężenia styczne na granicy rozkładu połączenia, c) przemieszczenia wypadkowe

In the model with veneering the CoCrMo framework with Duceram Kiss ceramics with the indenter load of 20N, the reduced stresses are located in the veneering layer and in the framework, with a characteristic spherical expansion after transition to the framework. In the veneering layer, the maximum value is 276.94 MPa (**Fig. 3b**). At the boundary of the layer connection, the reduced stresses are still high, i.e. in the range of 30–54.69 MPa. After transition to the CoCrMo framework, the values are in the range from 0.0541 MPa to 8 MPa. The shear stresses in the connection zone of the veneering layer and the framework range from -1.52 MPa to 1.58 MPa (**Fig. 3b**). The resultant displacements with a maximum value of 1.09 µm are located in the veneering zone with a minimal residual impact in the framework (**Fig. 3c**). In a small area, the stresses pass into the framework and reach the range of 0.05 µm to 0.13 µm. With such a configuration of the strength parameters for the veneering layer and the framework, a significant suppression of the displacements propagation was found in the framework.

In the Duceram Kiss – CoCrMo connection, when the load was increased from 5 N to 20 N, a characteristic peripheral peak of reduced stresses was noted on the border of the veneering layer and the framework: a larger area in the veneering layer, a shorter reach after transition to the framework which could cause the ceramics to chip off. It can be observed that, with the low flexibility of the framework (Young's modulus 203.8 GPa), there is a suppression of the resultant displacements.

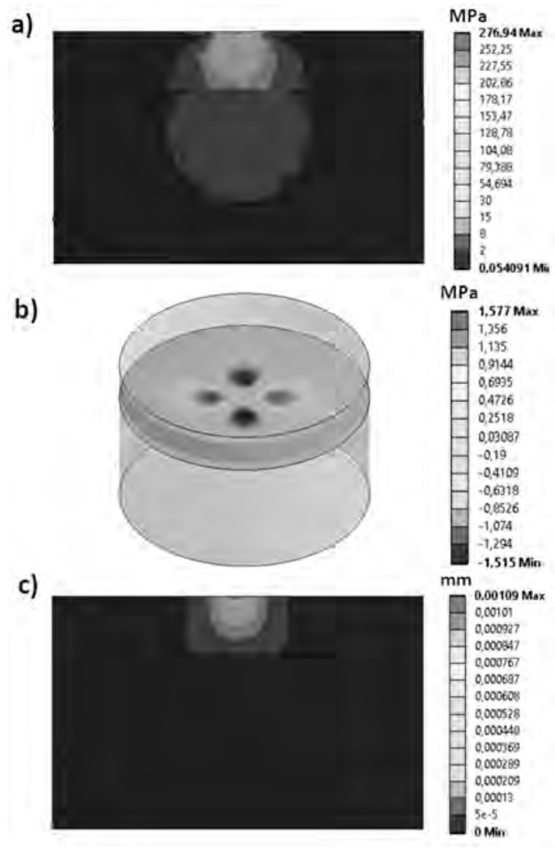

Fig. 3. Duceram Kiss-CoCrMo connection loaded with a force of 20 N: a) reduced stresses, b) shear stresses at the border of connection, c) resultant displacements

Rys. 3. Połączenie Duceram Kiss-CoCrMo obciążone siłą 20 N: a) naprężenia zredukowane, b) naprężenia styczne na granicy rozkładu połączenia, c) przemieszczenia wypadkowe

When veneering with Vita Titankeramic TiCP frameworks, with an indenter load of 5 N, the distribution of reduced stressed is characterized by the following values: maximum stress – 87.74 MPa, at the boundary of the layers the values drop to 2 MPa (**Fig. 4a**). In the titanium framework, the stresses show a minimum of 0.0069 MPa. The shear stresses in the connection zone between the veneering layer and the framework range from -0.23 MPa to 0.22 MPa (**Fig. 4b**). The resultant displacements are located both in the veneering layer and in the framework. The maximum values of 0.30 µm are obtained in the veneering layer. At the Vita

Titankeramik-TiCP boundary, the values are of 0.016 μm to 0.050 μm (**Fig. 4c**).

With a load of the indenter of 20 N, the distribution of reduced stresses when veneering the TiCP framework with Vita Titankeramik ceramics is characterized by the following values: maximum stress is 280.02 MPa, at the boundary of the layers the values decrease to 15–30 MPa (**Fig. 5a**). In the veneering layer, in the transition zone between the layers, there is a characteristic low concentration of reduced stresses of 30–55 MPa. The minimum stresses of 0.0046 MPa propagate within the titanium framework. The shear stresses in the connection zone of the veneering layer and the framework range from -1.71 MPa to 1.76 MPa (**Fig. 5b**). The resultant displacements with a maximum value of 0.81 μm are located in the veneering zone. At the Vita Titankeramik-TiCP boundary and in the framework, the values range from 0.05 μm to 0.11 μm (**Fig. 5c**). It can be observed that the TiCP framework slightly suppresses the propagation of displacements.

When veneering the Ti6Al4V framework with Vita Titankeramic ceramics with the indenter load of 5N,

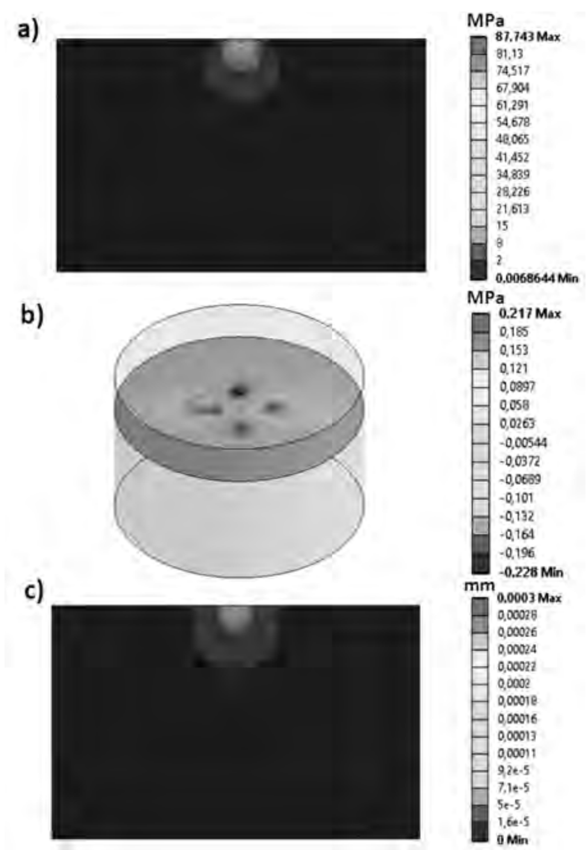

Fig. 4. Vita Titankeramik-TiCP connection loaded with a force of 5 N: a) reduced stresses, b) shear stresses at the border of connection, c) resultant displacements

Rys. 4. Połączenie Vita Titankeramik-TiCP obciążone siłą 5 N: a) naprężenia zredukowane, b) naprężenia styczne na granicy rozkładu połączenia, c) przemieszczenia wypadkowe

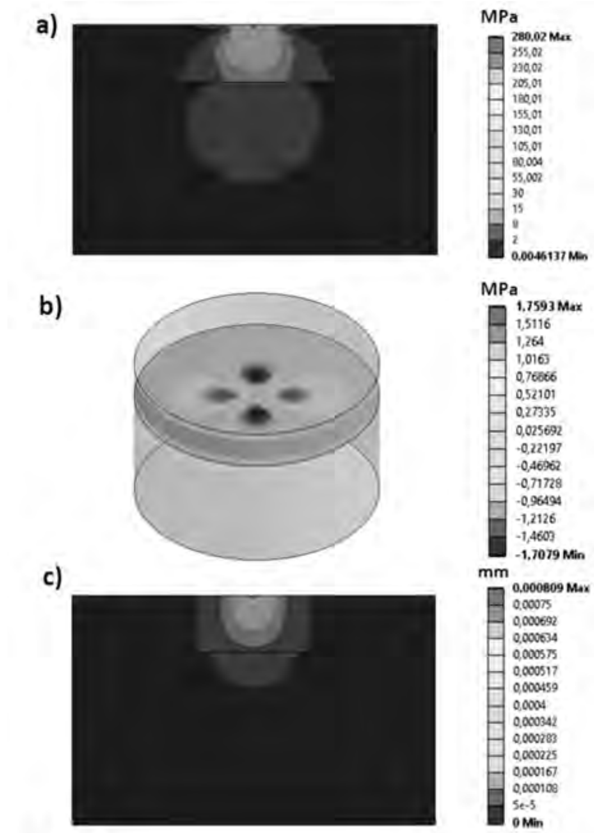

Fig. 5. Vita Titankeramik-TiCP connection loaded with a force of 20 N: a) reduced stresses, b) shear stresses at the border of connection, c) resultant displacements

Rys. 5. Połączenie Vita Titankeramik-TiCP obciążone siłą 20 N: a) naprężenia zredukowane, b) naprężenia styczne na granicy rozkładu połączenia, c) przemieszczenia wypadkowe

the distribution of reduced stresses is characterized by the following values: maximum stress is 87.77 MPa, at the boundary of the layers the value drops to 2 MPa (**Fig. 6a**). In the Ti6Al4V framework, minimum stresses are 0.0065 MPa. The shear stresses in the connection zone of the veneering layer and the framework range from -0.23 MPa to 0.22 MPa (**Fig. 6b**). The resultant displacements are located both in the veneering layer and in the framework. The maximum values of 0.30 μm are obtained in the veneering zone. At the Vita Titankeramik-Ti6Al4V boundary, the values are from 0.016 μm to 0.038 μm (**Fig. 6c**).

With the load of the indenter of 20 N, the distribution of reduced stresses when veneering the Ti6Al4V framework with Vita Titankeramik ceramics is characterized by the following values: the maximum stresses are 279.37 MPa, at the boundary of the layers the values decrease to 15–30 MPa (**Fig. 7a**). In the veneering layer, in the transition zone between the layers, there is a characteristic low concentration of reduced stresses of 30–54.94 MPa. In the Ti6Al4V framework,

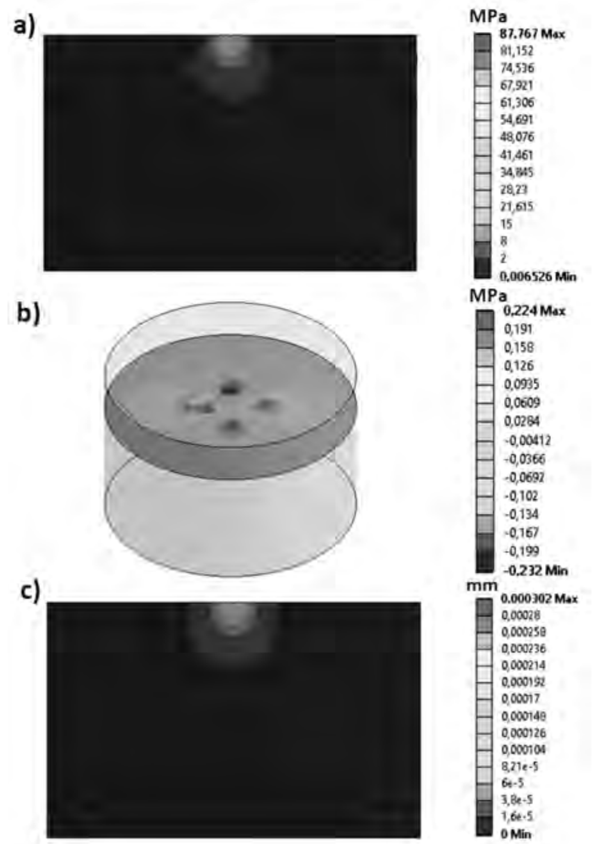

Fig. 6. Vita Titankeramik-Ti6Al4V connection loaded with a force of 5 N: a) reduced stresses, b) shear stresses at the border of connection, c) resultant displacements

Rys. 6. Połączenie Vita Titankeramik-Ti6Al4V obciążone siłą 5 N: a) naprężenia zredukowane, b) naprężenia styczne na granicy rozkładu połączenia, c) przemieszczenia wypadkowe

minimum stresses are 0.0024 MPa. The shear stresses in the connection zone between the veneering layer and the framework range from -1.69 MPa to 1.74 MPa (**Fig. 7b**). The resultant displacements with a maximum value of 0.81 µm are located in the veneering zone. At the Vita Titankeramik-Ti6Al4V boundary and in the framework, the values range from 0.05 µm to 0.11 µm (**Fig. 7c**).

There are small differences in the distribution of stresses and displacements in the connection of Vita Titankeramik ceramics and TiCP and Ti6Al4V frameworks. With the load of the indenter of 5 N, there is a slight transfer of reduced stresses to the framework – slightly higher with TiCP, probably due to a slightly lower value of the elasticity modulus. When the load is increased to 20 N, the reduced stresses spread gently within the TiCP and Ti6Al4V frameworks.

When veneering the glass-ceramic $LiSi_2$ framework with IPS e.max Ceram ceramics and the indenter load of 5 N, the distribution of reduced stresses is characterized by the following values: maximum stress is 109.96 MPa, at the boundary of the layers, the values decrease to 2 MPa (**Fig. 8a**). In the glass-ceramic framework, minimum stress is 0.0085 MPa. The shear stresses in the connection zone of the veneering layer and the framework range from -0.17 MPa to 0.18 MPa (**Fig. 8b**). The resultant displacements are located both in the veneering layer and in the framework. Maximum values of 0.30 µm are obtained in the veneering zone. At the IPS e.max Ceram-$LiSi_2$ boundary, the values are from 0.016 µm to 0.038 µm (**Fig. 8c**).

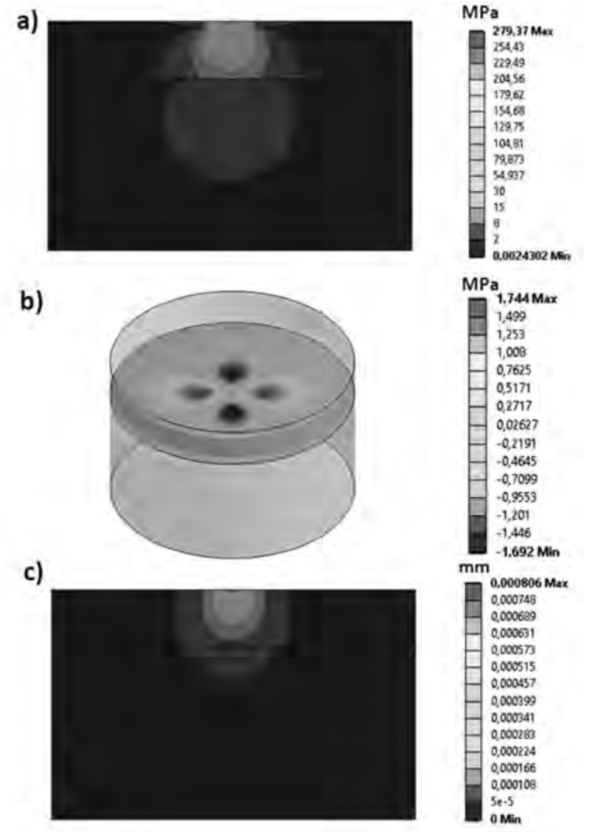

Fig. 7. Vita Titankeramik-Ti6Al4V connection loaded with a force of 20 N: a) reduced stresses, b) shear stresses at the border of connection, c) resultant displacements

Rys. 7. Połączenie Vita Titankeramik-Ti6Al4V obciążone siłą 20N : a) naprężenia zredukowane, b) naprężenia styczne na granicy rozkładu połączenia, c) przemieszczenia wypadkowe

With the indenter load of 20 N, the distribution of reduced stresses when veneering the glass-ceramic $LiSi_2$ framework with IPS e.max Ceram ceramics is characterized by the following values: maximum stress – 292.06 MPa, and at the boundary of the layers, the values drops to 15–30 MPa (**Fig. 9a**). In the veneering layer, in the transition zone between the layers, there is a small area of very little concentration of reduced stresses of 30–56.21 MPa. In the glass-ceramic framework, minimum stress is 0.0564 MPa. The shear stresses in the connection zone of the veneering layer and the framework range from -1.80 MPa to 1.81 MPa

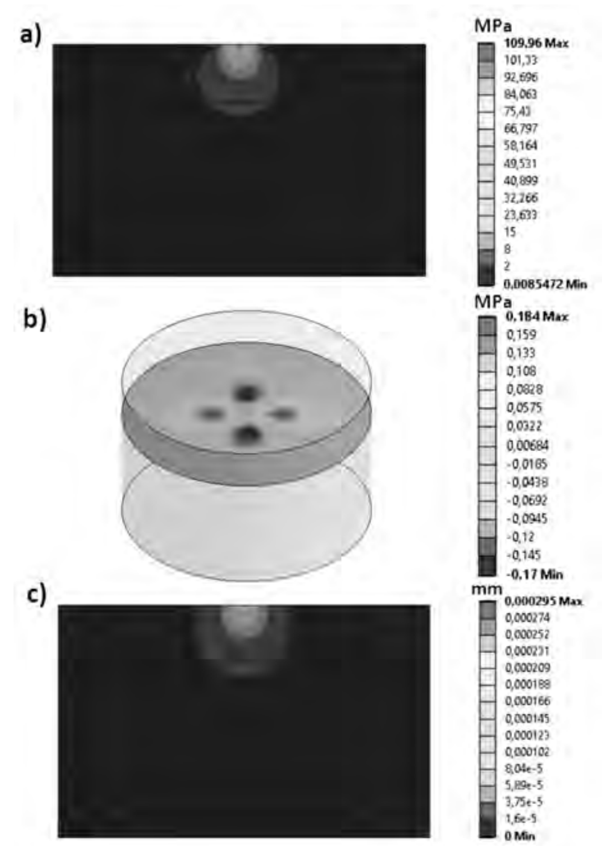

Fig. 8. IPS e.max Ceram-LiSi$_2$ connection loaded with a force of 5 N: a) reduced stresses, b) shear stresses at the border of connection, c) resultant displacements

Rys. 8. Połączenie IPS e.max Ceram-LiSi$_2$ obciążone siłą 5 N: a) naprężenia zredukowane, b) naprężenia styczne na granicy rozkładu połączenia, c) przemieszczenia wypadkowe

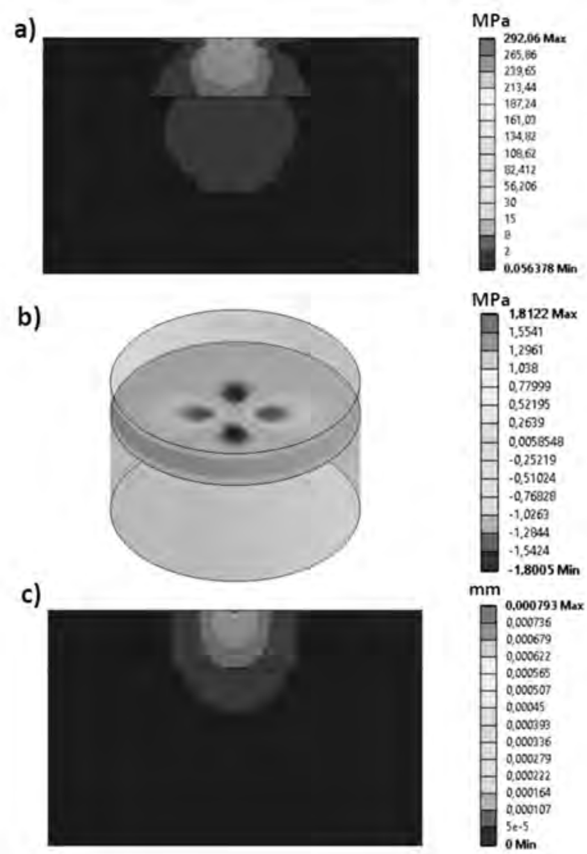

Fig. 9. IPS e.max Ceram-LiSi$_2$ connection loaded with a force of 20 N: a) reduced stresses, b) shear stresses at the border of connection, c) resultant displacements

Rys. 9. Połączenie IPS e.max Ceram-LiSi$_2$ obciążone siłą 20 N: a) naprężenia zredukowane, b) naprężenia styczne na granicy rozkładu połączenia, c) przemieszczenia wypadkowe

(**Fig. 9b**). The resultant displacements with a maximum value of 0.79 µm are located in the veneering layer. At the border of IPS e.max Ceram-LiSi$_2$ and in the framework, there are values of 0.05 µm to 0.11 µm (**Fig. 9c**). It can be observed that the LiSi$_2$ framework slightly suppresses the propagation of displacements.

In the material composition of IPS e.max Ceram-LiSi$_2$, both load variants of 5 N and 20 N show very high values of reduced stresses and their concentration in the superficial zone. Particularly high values of the stresses were found for veneering with IPS e.max Ceram (with the modulus of elasticity of 95 MPa) of the LiSi$_2$ glass-ceramic framework (with the modulus of also 95 MPa). This nature of the connection is unfavourable in terms of strength.

In the model with veneering the ZrO$_2$ framework with Elephant Sakura ceramics and a 5 N indenter load, the reduced stresses are located in the veneering layer and in the framework, with a characteristic expansion after transition to the framework. In the veneering layer, the values range from 90.34 MPa – the maximum value, to 2 MPa (**Fig. 10a**). At the boundary of the layers, the stresses are of 2–8 MPa. After the transition to the zirconium framework, the values reach a minimum of 0.0014 MPa. The shear stresses in the connection zone of the veneering layer and the framework range from -0.26 MPa to 0.29 MPa (**Fig. 10b**). The resultant displacements with a maximum value of 0.45 µm are located only in the veneering layer (**Fig. 10c**). With such a configuration of strength parameters of the veneering layer and the framework, the propagation of displacements was suppressed. This is a favourable phenomenon that ensures good adhesion of the veneering ceramics to the framework.

In the model with veneering ZrO$_2$ framework with Elephant Sakura ceramics and an indenter load of 20 N, the reduced stresses are located in the veneering layer and in the framework, with a characteristic expansion after transition to the framework. In the veneering layer, the values start with 280.07 MPa – the maximum

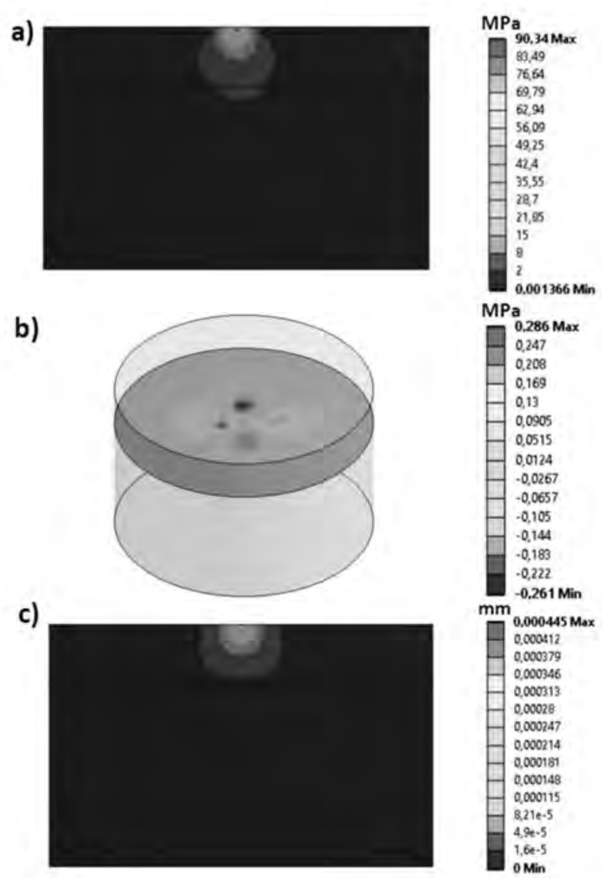

Fig. 10. Elephant Sakura-ZrO_2 connection loaded with a force of 5 N: a) reduced stresses, b) shear stresses at the border of connection, c) resultant displacements

Rys. 10. Połączenie Elephant Sakura-ZrO_2 obciążone siłą 5 N: a) naprężenia zredukowane, b) naprężenia styczne na granicy rozkładu połączenia, c) przemieszczenia wypadkowe

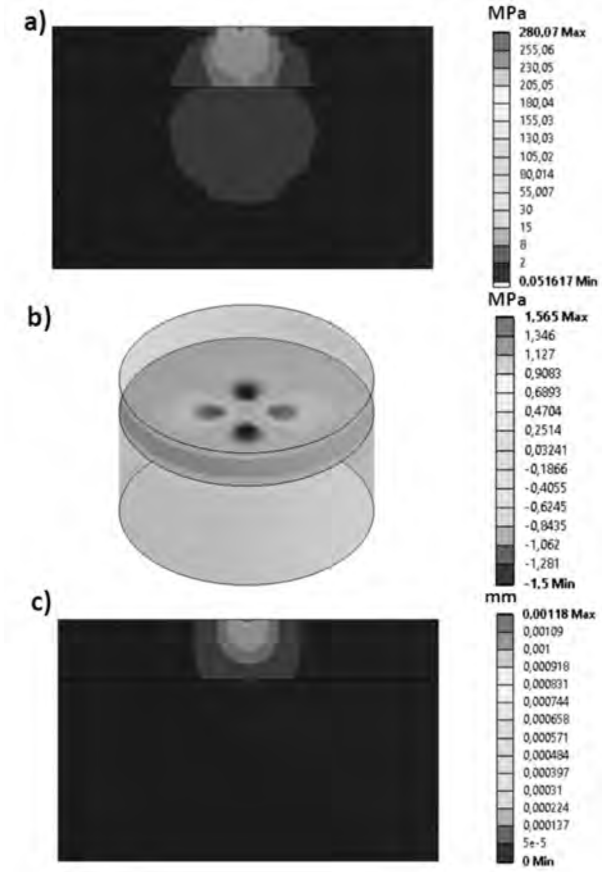

Fig. 11. Elephant Sakura-ZrO_2 connection loaded with a force of 20 N: a) reduced stresses, b) shear stresses at the border of connection, c) resultant displacements

Rys. 11. Połączenie Elephant Sakura-ZrO_2 obciążone siłą 20 N: a) naprężenia zredukowane, b) naprężenia styczne na granicy rozkładu połączenia, c) przemieszczenia wypadkowe

value, at the border of the layers the values decrease to 8–15 MPa (**Fig. 11a**). However, in the veneering layer, in the transition zone between the layers, there is a small area with the value of reduced stresses in the range of 30–55.01 MPa. After transition to the zirconium framework, the values reach a minimum of 0.0516 MPa. The shear stresses in the connection zone of the veneering layer and the framework range from -1.50 MPa to 1.57 MPa (**Fig. 11b**). The resultant displacements with a maximum value of 1.18 μm are located in the veneering layer (**Fig. 11c**). In a small area, the stresses pass into the framework and reach the values from 0.05 μm to 0.14 μm. With such a configuration of the strength parameters of the veneering layer and the framework, a significant suppression of the propagation of displacements was found in the framework.

For the composite-PEEK material composition and the indenter load of 5 N, the maximum reduced stress is 86.99 MPa (**Fig. 12a**). Moving closer to the boundary of the framework, the stresses decrease to 2 MPa. The minimum value in the PEEK framework is 0.0208 MPa. The selected shear stresses at the connection of the veneering layer and the framework remain in the range from -0.10 MPa to 0.11 MPa (**Fig. 12b**). The resultant displacements spread smoothly from the place of contact with the indenter and have a maximum value of 2.07 μm, and, at the composite-PEEK border, the values are from 0.39 μm to 0.54 μm (**Fig. 12c**). The displacements are suppressed in the framework.

With a load of the indenter of 20 N, in the composite-PEEK material composition, the maximum reduced stress is 263.09 MPa (**Fig. 13a**). In the veneering layer, in the transition zone between layers, there is an area with reduced stresses in the range of 15–30 MPa. In the composite, there is a characteristic concentric propagation of HMH stresses in the superficial layer of the composite and in the vicinity of the composite-PEEK boundary. The minimum value in the PEEK

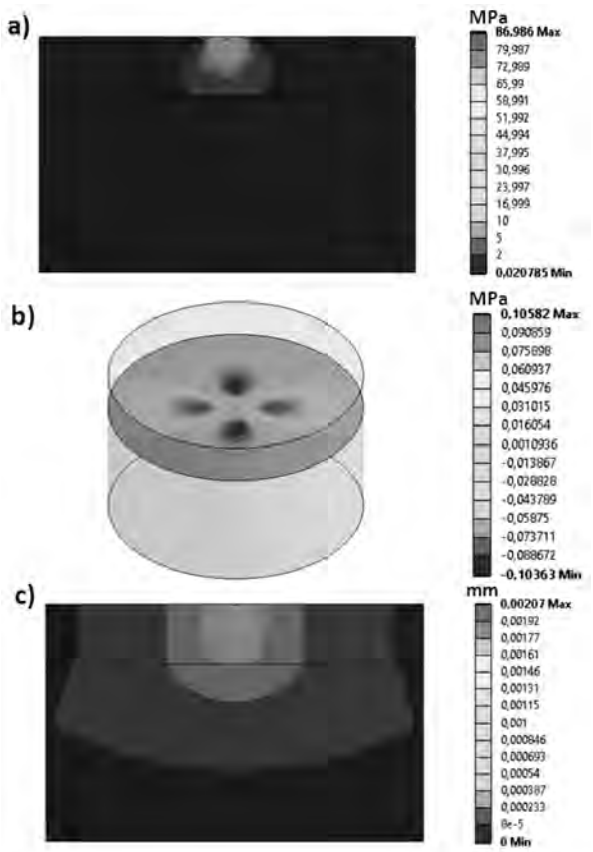

Fig. 12. Composite-PEEK connection loaded with a force of 5 N: a) reduced stresses, b) shear stresses at the border of connection, c) resultant displacements

Rys. 12. Połączenie kompozyt-PEEK obciążone siłą 5 N: a) naprężenia zredukowane, b) naprężenia styczne na granicy rozkładu połączenia, c) przemieszczenia wypadkowe

framework is 0.1203 MPa. The selected shear stresses at the connection of the veneering layer and the framework are in the range from -2.43 MPa to 2.34 MPa (**Fig. 13b**). The resultant displacements spread smoothly from the point of contact with the indenter and have a maximum value of 6.04 µm, and, at the composite-PEEK border, the values are from 2.07 µm to 2.51 µm (**Fig. 13c**). It can be noticed that the PEEK framework slightly suppresses the propagation of displacements.

In the enamel-dentin connection, with the load of the indenter 5 N, reduced stresses with a maximum value of 81.78 MPa are located in direct contact with the indenter (**Fig. 14a**). The stresses are generated towards the inside of the enamel layer starting from the area of maximum stress and reduce their values to 2 MPa. The minimum reduced stresses in the dentine reach the value of 0.0158 MPa. The shear stresses at the junction of the enamel and dentin are small, ranging from -0.10 MPa to 0.11 MPa (**Fig. 14b**). The resultant displacements with a maximum value of 0.37 µm gently pass from the enamel to the dentin with the values from 0.10 µm to 0.13 µm, stimulating dentinal tubules (**Fig. 14c**).

With an indenter load of 20 N, in the enamel-dentin junction, reduced stresses with a maximum value of 260.67 MPa are located in direct contact with the indenter (**Fig. 15a**). In the veneering layer, in the transition zone between layers, there is an area with reduced stresses in the range of 15–30 MPa. In the enamel, there is a characteristic concentric distribution of HMH stresses in the superficial layer of the enamel and in the vicinity of the enamel-dentin junction. The minimum reduced stress in the dentin is 0.118 MPa. The shear stresses at the junction of the enamel and dentin range from -2.49 MPa to 2.38 MPa (**Fig. 15b**). The resultant displacements with a maximum value of 1.07 µm gently pass from the enamel to the dentin with the values from 0.37 µm to 0.45 µm, stimulating dentinal tubules (**Fig. 15c**). It can be noticed that the dentine slightly suppresses the propagation of displacements.

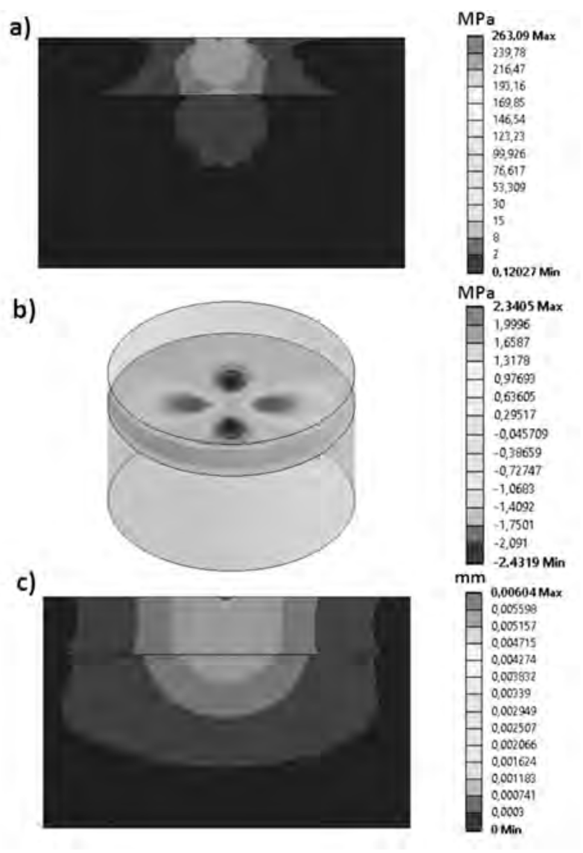

Fig. 13. Composite-PEEK connection loaded with a force of 20 N: a) reduced stresses, b) shear stresses at the border of connection, c) resultant displacements

Rys. 13. Połączenie kompozyt-PEEK obciążone siłą 20 N: a) naprężenia zredukowane, b) naprężenia styczne na granicy rozkładu połączenia, c) przemieszczenia wypadkowe

In the natural enamel-dentin junction, with a relatively low value of the dentin elasticity modulus and about 4 times higher value of the enamel elasticity modulus, the resultant displacements have a large area

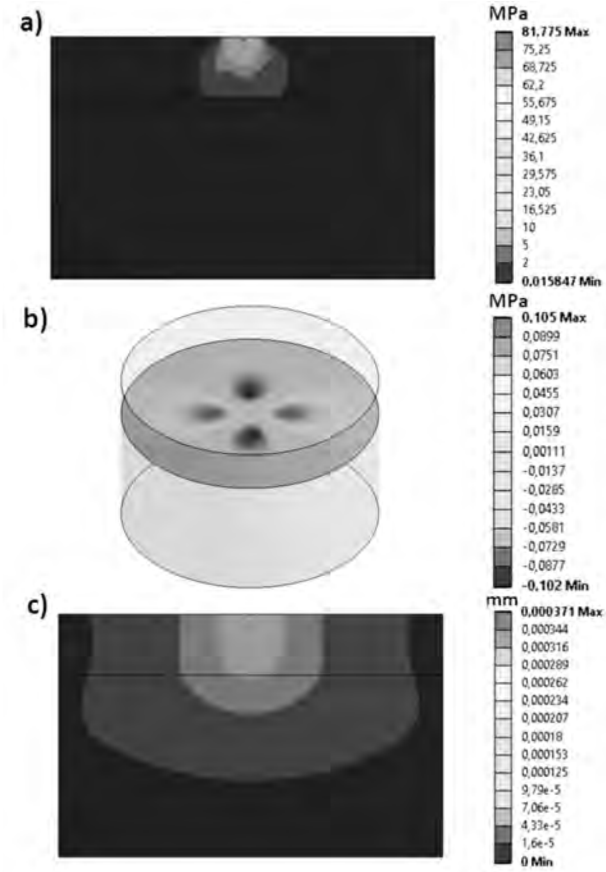

Fig. 14. Enamel-dentin connection loaded with a force of 5 N: a) reduced stresses, b) shear stresses at the border of connection, c) resultant displacements

Rys. 14. Połączenie szkliwno-zębinowe obciążone siłą 5 N: a) naprężenia zredukowane, b) naprężenia styczne na granicy rozkładu połączenia, c) przemieszczenia wypadkowe

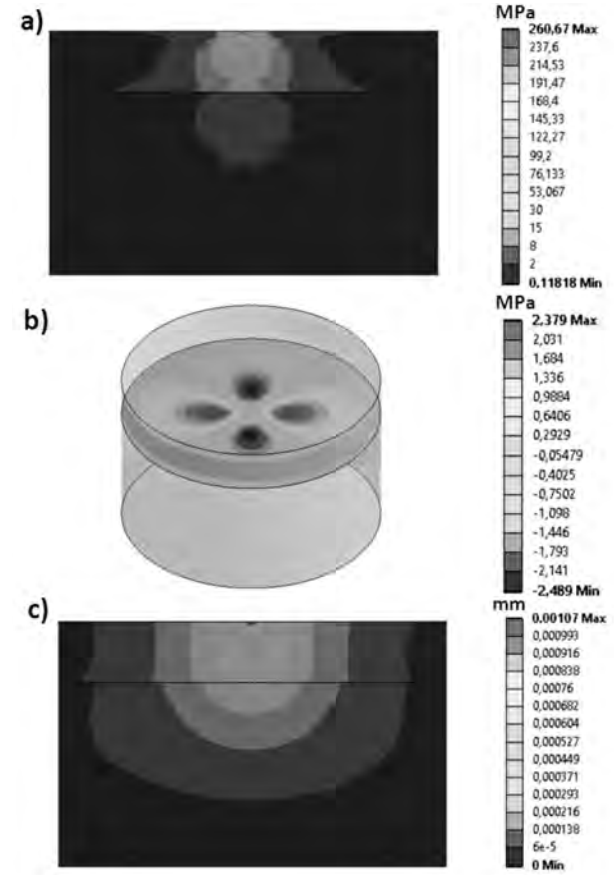

Fig. 15. Enamel-dentin connection loaded with a force of 20 N: a) reduced stresses, b) shear stresses at the border of connection, c) resultant displacements

Rys. 15. Połączenie szkliwno-zębinowe obciążone siłą 20 N: a) naprężenia zredukowane, b) naprężenia styczne na granicy rozkładu połączenia, c) przemieszczenia wypadkowe

of propagation and small values. At the same time, high values of shear stresses can be noticed. The nature of the connection between the enamel prisms and dentin, with significant stress values, stimulates the pulp fluid in the tubular structure of the dentin.

The simulation examinations performed in concentrated contact of layered material compositions used for prosthetic crowns give better differentiation of results with the load of the indenter of 20 N. This load allows for correlation with the pressures that occur in the stomatognathic system during chewing.

The load-bearing layer with a high value of Young's modulus (CoCrMo, ZrO_2) limits the spread of resultant displacements to the framework to the greatest extent. However, there are quite significant values of shear stresses at the border of the veneering layer and the framework. These shear stress values may deteriorate the adhesion of the veneering layer to the framework in the ceramic-metal composition (material diversity). They do not cause negative effects in ceramics-ceramics compositions.

In the load-bearing layers made of TiCP and Ti6Al4V, there is a limited spread of resultant displacements into the framework, but there are significant values of shear stresses at the connection boundary. These significant shear stress values can adversely affect the adhesion of the ceramics to titanium and its alloys.

In the ceramics-ceramics and ceramics-glass ceramics compositions, creating a permanent adhesive bond is much easier than in the ceramics-metal composition because of material diversity.

It should be noted that, for the IPS e.max Ceram-$LiSi_2$ composition, the high value of the elasticity modulus for the veneering layer, even under the load of 5 N, gives the highest concentration of reduced stresses in the near-surface zone. These stresses can adversely affect the opposing teeth, especially if they are natural. The stresses can damage the enamel of these teeth.

Given the development of biomaterials and technologies used for the production of fixed prosthetic restorations, the layered structure with Elephant Sakura veneering on the ZrO_2 framework will be the most optimal solution.

In the PEEK framework with very high elasticity, veneered with composite, the resultant displacements have a very large area of propagation and very high values. In this material composition, the highest values of shear stresses occur at the connection of the veneering layer and the framework. The more elastic the load-bearing layer is, the greater are the shear stresses.

The tests were carried out in concentrated contact on samples that had not been subjected to previous loads or tribological wear. Under chewing conditions, wear occurs and the contact surface may increase. In such a situation, the values of stresses and displacements could decrease.

CONCLUSIONS

With significant material differentiation and various strengths of the layers making up the material compositions of prosthetic crowns, the FEM analysis is an objective tool for assessing resistance of the materials and demonstrating the impact of strength parameters of the veneering layer and the framework on the transfer of external loads.

If the material building the veneering layer differs from the material of the framework, for example, in the ceramic-metal type, spreading of the resultant displacements to the framework and high values of shear stress at the border of the veneering layer and the framework may be unfavourable factors causing the veneering layer to chip off. Such distribution of stresses and displacements may have a much smaller impact on the veneering of a ceramic or glass-ceramic framework, as both layers are much more homogeneous in terms of the material composition.

In layered ceramic-metal and ceramic-zirconium oxide compositions, there is a phenomenon of limiting the area of stress and displacement propagation with increased values of the framework elasticity modulus.

It should be emphasized that, in the case of crowns constituting the pillars of extensive bridges, frameworks made of metal or its alloys are a very good solution in terms of strength, especially commonly used cobalt-chromium frameworks, which may differ in terms of aesthetics and biocompatibility from all-ceramic restorations, but the veneering procedure ensures a good adhesive bond under changing loads.

A zirconium oxide framework veneered with Elephant Sakura ceramics is the most optimal solution in terms of strength, aesthetics, and biocompatibility.

ACKNOWLEDGEMENT

This work is financed by AGH University of Science and Technology, Faculty of Mechanical Engineering and Robotics: subvention No. 16.16.130.942.

REFERENCES:

1. Malara P., Paluch K., Sobolewska K., Pasieka A.: The study of the connection between the zirconia substructure and veneering porcelain in dental crowns subjected to occlusal forces. Archives of Materials Science, 6 (2016), p. 6.
2. Toussi C.A., Ezatpour H.R., Haddadnia J., Shiri J.G.: Effect of using different metal and ceramic materials as restorations on stress distribution around dental implants: a comparative finite element study. Materials Research Express, 5, 11 (2018), p. 115403.
3. Malara P., Paluch K., Sobolewska K., Pasieka A.: Assessment of the compressive strength of the metal-ceramic connections in fixed dental restorations. Journal of Achievements in Materials and Manufacturing Engineering, 79, 2 (2016), pp. 66–73.
4. Ryniewicz W., Ryniewicz A.M.: Model analysis of the stomatognathic system restorations using prosthetic bridges. Przegląd Elektrotechniczny, 91, 5 (2015), pp. 17–20.
5. Bojko Ł., Ryniewicz W., Ryniewicz A.M., Kot M., Pałka P.: The influence of additive technology on the quality of the surface layer and the strength structure of prosthetic crowns. Tribologia, 4 (2018), pp. 13–22.
6. Zaher A.M., Hochstedler J.L., Rueggeberg F.A., Kee E.L.: Shear bond strength of zirconia–based ceramics veneered with 2 different techniques. The Journal of prosthetic dentistry, 118, 2 (2017), pp. 221–227.
7. Kirmali O., Kapdan A., Kustarci A., Er K.: Veneer ceramic to Y–TZP bonding: comparison of different surface treatments. Journal of Prosthodontics, 25, 4 (2016), pp. 324–329.
8. Fukuyama T., Hamano N., Ino S.: Effects of silica-coating on surface topography and bond strength of porcelain fused to CAD/CAM pure titanium. Dental materials journal, 35, 2 (2016), pp. 325–332.
9. Bae E.J., Kim H.Y., Kim W.C., Kim J.H.: In vitro evaluation of the bond strength between various ceramics and cobalt-chromium alloy fabricated by selective laser sintering. The journal of advanced prosthodontics, 7, 4 (2015), pp. 312–316.

10. Han X., Sawada T., Schille C., Schweizer E., Scheideler L., Geis-Gerstorfer J., Spintzyk S.: Comparative analysis of mechanical properties and metal-ceramic bond strength of Co-Cr dental alloy fabricated by different manufacturing processes. Materials, 11, 10 (2018), p. 1801.
11. Ryniewicz W., Ryniewicz A.M., Bojko Ł.: The effect of a prosthetic crown's design on the accuracy of mapping an abutment teeth's shape. Measurement, 91 (2016), pp. 620–627.
12. Ryniewicz A.M., Bojko Ł., Ryniewicz W.I.: Microstructural and micromechanical tests of titanium biomaterials intended for prosthetic reconstructions. Acta of bioengineering and biomechanics, 18, 1(2016), pp. 121–127.
13. Nguyen H.H., Wan S., Tieu K.A., Pham S.T., Zhu, H.: Tribological behaviour of enamel coatings. Wear, 426 (2019), pp. 319–329.
14. Bojko Ł., Ryniewicz W., Ryniewicz A.M., Kot M.: Study of the impact of incremental technology on mechanical and tribological properties of biomaterials. Tribologia, 3 (2017), pp. 29–38.
15. Kaleli N., Sarac D., Külünk S., Öztürk Ö.: Effect of different restorative crown and customized abutment materials on stress distribution in single implants and peripheral bone: A three-dimensional finite element analysis study. The Journal of prosthetic dentistry, 119, 3 (2018), pp. 437–445.
16. Tribst J.P.M., Dal Piva A.M.D.O., Penteado M.M., Borges A.L.S., Bottino M.A.: Influence of ceramic material, thickness of restoration and cement layer on stress distribution of occlusal veneers. Brazilian oral research, 32 (2018).
17. Archangelo C.M., Rocha E.P., Anchieta R.B., Martin M., Freitas A.C., Ko C.C., Cattaneo P.M.: Influence of buccal cusp reduction when using porcelain laminate veneers in premolars. A comparative study using 3-D finite element analysis. Journal of Prosthodontic Research, 55, 4 (2011), pp. 221–227.
18. De Kler M., De Jager N., Meegdes M., Van Der Zel J.M.: Influence of thermal expansion mismatch and fatigue loading on phase changes in porcelain veneered Y-TZP zirconia discs. Journal of oral rehabilitation, 34, 11 (2007), pp. 841–847.